Karl-Franzens-Universität Graz

Bachelor Thesis

The Aharonov-Bohm-Effect

Author:
Oliver Orasch

Supervisor:
Ao. Univ. Prof. Dr.
Ulrich Hohenester

December 16, 2014

Contents

Preface

This thesis sums up the theoretical prediction and the experimental confirmation of the so-called Aharonov-Bohm-Effect [AB-Effect]. With their work Yakir Aharonov and David Bohm revolutionized the role of electromagnetic potentials in physics. To show that, simple demonstrative examples, groundbreaking experiments, as well as applications will be presented.

The thesis is divided in three major chapters. We start with a section, which describes the required theory to understand the processes associated with the AB-effect. It covers the gauge transformation, the basic quantum mechanics and further examples, which point out the consequences of electromagnetic potentials. Concluding this chapter, the main work of Aharonov and Bohm will be presented.

The second chapter concentrates on the experimental confirmation of the AB-effect, respectively on the attempts to show the influence of electromagnetic potentials. Starting with the early experiments of Chambers and Möllenstedt and Bayh, using mainly electron biprisms, we end up at Tonomura's set-ups, where "electron- and optical-holographic techniques [were] employed". [5]

Concluding this thesis the last chapter deals with one application of the AB-effect. The consequences of miniaturization - in reference to the AB-effect - will be shown.

Oliver Orasch Graz, December 16, 2014

Symbols and units

Common symbols used during the thesis:

$\vec{A}(\vec{x},t)$ ... vector potential on location $\vec{x}$

$\vec{B}(\vec{x},t)$ ... magnetic field on location $\vec{x}$

$\phi(\vec{x},t)$ ... electrostatic potential on location $\vec{x}$

$\vec{E}(\vec{x},t)$ ... magnetic field on location $\vec{x}$

$\Delta\varphi$ ... relative phase shift/ phase difference

ϕ ... magnetic flux through a surface σ

$\hat{H}_0$ ... Hamiltonian in a region without electromagnetic potentials or fields

$\hat{H}$ ... general Hamiltonian

e_0 ... unit charge

$e = -e_0$ ... charge of an electron

c ... velocity of light

$\hbar$ ... reduced Planck constant

i ... imaginary unit

$\psi_0(\vec{x},t)$ ... wave function for regions without electromagnetic potentials or fields

$\psi(\vec{x},t)$ ... general wave function

Ψ ... composit wave function

$\Lambda(\vec{x},t)$ ... arbitrary gauge function

Due to the appearance of electrodynamics, the Gaussian unit system will be used. That means

$$[\phi(\vec{x},t)] = \left[\vec{A}(\vec{x},t)\right] \quad \text{and} \quad \left[\vec{B}(\vec{x},t)\right] = \left[\vec{E}(\vec{x},t)\right],$$

where "[...]" denotes the unit of a physical quantity. [12]

1 AB-Effect: Theory

1.1 Introduction

In 1959 Aharonov and Bohm published a paper with the title "Significance of Electromagnetic Potentials in the Quantum Theory". They predicted that electromagnetic potentials ϕ and $\vec{A}$ might be real physical quantities and that this could be shown in electron interference experiments. [1]

The AB-Effect is merely a phenomenon of quantum mechanics, which is described by the Hamilton formalism. Contrary to Newtonian mechanics, where the electromagnetic fields are used via

$$\vec{B} = \vec{\nabla} \times \vec{A} \tag{1}$$

and

$$\vec{E} = -\frac{1}{c}\frac{\partial \vec{A}}{\partial t} - \vec{\nabla}\phi, \tag{2}$$

the Hamiltonian formulation allows only the pure electromagnetic potentials in the equations of motion. [12] [11]

In classical mechanics and electrodynamics potentials are more or less used to simplify calculations. [13] However, it is always possible to compute a solution using the electromagnetic fields instead. [19] The fact that Newton's and Hamilton's formulations of mechanics have to be equal for classical mechanics, explains why the AB-effect did not show up before quantum mechanics.

To demonstrate Aharonov and Bohm's statement, the first experiments focusing only on the magnetic AB-effect were realized by Chambers in 1960 and by Möllenstedt and Bayh in 1962. [4,16,19] These experiments showed for the first time that the vector potential $\vec{A}$ has a direct influence on the electron dynamics and causes fringe shifts in the interference pattern. However, Aharonov and Bohm criticized such settings in their second paper, because the magnetic field $\vec{B}$ and the vector potential $\vec{A}$ were not separated adequately. [2]

In the 1980's Akira Tonomura and his team gave solid evidence. They arranged highly sophisticated experiments to get a situation where only a vector potential but no magnetic field is present. [5,6]

The development of the theory and the search for experimental confirmation of Aharonov and Bohm's calculations is far more than an episode of science history. The AB-effect and its applications are a current issue of modern nanoscience. [17] In Murray Peshkin's words,"The experimental quantization of the fluxoid in superconducting rings and Josephson junctions has been interpreted as an experimental confirmation of AB effect". [19]

1.2 Hamiltonian for e.m. problems

To quote Richard Feynman, "Know your Hamiltonian!" [10], it is very revealing to analyze the workhorse of non-relativistic quantum mechanics. Therefore we start at the very beginning, at classical mechanics. The Hamilton-function in classical mechanics is equal to the energy of the system,

$$H = T + V. \tag{3}$$

This holds for arbitrary potentials V that are independent of the particle velocity, whereas the kinetic energies T depend quadratically on it. [11] In general, the Hamiltonian-function can be written as

$$H = \frac{\vec{p}^{\,2}}{2m} + V(\vec{x}), \tag{4}$$

with the momentum $\vec{p}$ and the particle mass m.

To apply the classical Hamilton-function to quantum mechanics, one has to replace the variables $\vec{p}$ and $\vec{x}$ by operators, which will be denoted by a "hat" on top of the variable.

In general the Hamilton-operator (Hamiltonian) takes the form

$$\hat{H} = \frac{\hat{\vec{p}}^{\,2}}{2m} + V(\vec{x}), \quad \text{with} \quad \hat{\vec{p}} = \frac{\hbar}{i}\vec{\nabla}. \tag{5}$$

Applying the Hamiltonian to electromagnetic problems, the kinematic momentum has to be replaced by [21]

$$m\dot{\vec{x}} = \vec{p} - \frac{e}{c}\vec{A}, \tag{6}$$

where $\vec{p}$ is the canonical momentum and $\vec{A}$ the vector potential. Furthermore, the potential energy contribution has to be extended by $e\phi(\vec{x})$, which is the potential energy due to an electrostatic potential.
With the last replacements the Hamiltonian allows to treat arbitrary problems involving electromagnetic fields for a scalar particle, and transforms to [20]

$$\hat{H} = \frac{1}{2m}\left[\hat{\vec{p}} - \frac{e}{c}\vec{A}\right]^2 + e\phi(\vec{x}) + V(\vec{x}), \tag{7}$$

where $V(\vec{x})$ is an additional arbitrary contribution to the potential energy, which will be set to zero in the following.

Now we are able, to write down the general Schrödinger equation for purely electromagnetic problems.

$$i\hbar\frac{\partial}{\partial t}\psi(\vec{x},t) = \left[\frac{1}{2m}\left[\hat{\vec{p}} - \frac{e}{c}\vec{A}\right]^2 + e\phi(\vec{x})\right]\psi(\vec{x},t) \tag{8}$$

Due to the fact that we are only interested in field-free-regions, there does not enter a spin contribution.

1.3 Gauge Transformations

The fact that the electromagnetic fields are constructed by differential operators shows that the electromagnetic potential $A^\mu = \left(\phi, \vec{A}\right)$ is well defined up to the derivative of an arbitrary function $\partial^\mu \Lambda$. This property is called gauge freedom and has to be fixed, as we will see later. Due to the gauge properties of ϕ and $\vec{A}$, they are often called gauge fields. [9] These points will be described in more detail in the following.

1.3.1 General aspects

Generally, the curl of a conservative field vanishes [14],

$$\vec{\nabla} \times \left[\vec{\nabla}\Lambda(\vec{x}, t)\right] = 0. \tag{9}$$

Therefore the magnetic field $\vec{B}$ does not change under a gauge transformation of the form

$$\vec{A}(\vec{x}, t) \quad \longrightarrow \quad \vec{A}(\vec{x}, t) + \vec{\nabla}\Lambda(\vec{x}, t). \tag{10}$$

In this case, $\Lambda(\vec{x}, t)$ is an arbitrary and real scalar field, a so-called gauge function. [13]

To grant the same for the electric field

$$\vec{E} = -\frac{1}{c}\frac{\partial \vec{A}}{\partial t} - \vec{\nabla}\phi, \tag{11}$$

one has to insert (10) in (11).

$$\vec{E}' = -\frac{1}{c}\frac{\partial \vec{A}'}{\partial t} - \vec{\nabla}\phi' = -\frac{1}{c}\frac{\partial}{\partial t}\left[\vec{A} + \vec{\nabla}\Lambda\right] - \vec{\nabla}\phi' \stackrel{!}{=} \vec{E} \tag{12}$$

It follows that

$$\vec{E} = -\frac{1}{c}\frac{\partial \vec{A}}{\partial t} - \vec{\nabla}\left[\phi' + \frac{1}{c}\frac{\partial \Lambda}{\partial t}\right] \tag{13}$$

and the corresponding gauge transformation reads off as

$$\phi(\vec{x}, t) \quad \longrightarrow \quad \phi(\vec{x}, t) - \frac{1}{c}\frac{\partial \Lambda(\vec{x}, t)}{\partial t}. \tag{14}$$

In the language of 4-vectors, the gauge transformation of the electromagnetic fields becomes

$$A^\mu \longrightarrow A^\mu - \partial^\mu \Lambda,$$

with $A^\mu = \left(\phi, \vec{A}\right)$ and $\partial^\mu = \left(\frac{1}{c}\frac{\partial}{\partial t}, -\vec{\nabla}\right)$. [11]

1.3.2 Schrödinger equation

Next it is important to check what happens to the general Schrödinger equation, if a gauge transformation of the potentials is performed. Starting at

$$i\hbar\frac{\partial}{\partial t}\psi = \left[\frac{1}{2m}\left[\hat{p} - \frac{e}{c}\vec{A}\right]^2 + e\phi(\vec{x})\right]\psi, \tag{15}$$

we insert the transformed potentials $\vec{A}'$ and ϕ'.

$$i\hbar\frac{\partial}{\partial t}\psi =$$

$$= \left[\frac{1}{2m}\left(\hat{p} - \frac{e}{c}\vec{A}(\vec{x},t) - \frac{e}{c}\vec{\nabla}\Lambda(\vec{x},t)\right)^2 + e\left(\phi(\vec{x},t) - \frac{1}{c}\frac{\partial\Lambda(\vec{x},t)}{\partial t}\right)\right]\psi \tag{16}$$

$$i\hbar\left(\frac{\partial}{\partial t}\psi - \frac{ie}{c\hbar}\psi\frac{\partial\Lambda(\vec{x},t)}{\partial t}\right) =$$

$$= \left[\frac{1}{2m}\left(\hat{p} - \frac{e}{c}\vec{A}(\vec{x},t) - \frac{e}{c}\vec{\nabla}\Lambda(\vec{x},t)\right)^2 + e\phi(\vec{x},t)\right]\psi \tag{17}$$

A closer analysis of the l.h.s. of (17) shows that this part can also be transformed using

$$\psi = \psi' e^{-iS(\vec{x},t)}, \quad \text{with} \quad S(\vec{x},t) \equiv \frac{e}{\hbar c}\Lambda(\vec{x},t). \tag{18}$$

To show this, we take the time derivative of (18) and write explicitly

$$\frac{\partial}{\partial t}\psi = e^{-iS(\vec{x},t)}\frac{\partial}{\partial t}\psi' - \psi' i e^{-iS(\vec{x},t)}\frac{\partial}{\partial t}S(\vec{x},t) = \tag{19}$$

$$= \left[e^{-iS(\vec{x},t)}\frac{\partial}{\partial t} - ie^{-iS(\vec{x},t)}\frac{\partial}{\partial t}S(\vec{x},t)\right]\psi e^{iS(\vec{x},t)}. \tag{20}$$

Multiplying (19) to the left with $e^{iS(\vec{x},t)}$, we find

$$e^{iS(\vec{x},t)}\frac{\partial}{\partial t}\psi = \left[\frac{\partial}{\partial t} - i\frac{\partial}{\partial t}S(\vec{x},t)\right]\psi e^{iS(\vec{x},t)}. \tag{21}$$

By replacing the time derivatives in (21) by spatial ones, $\vec{\nabla}$ can be transformed too. In general such a transformation looks like [21]

$$e^{f(x)}\frac{\partial}{\partial x} = \left(\frac{\partial}{\partial x} - \frac{\partial f}{\partial x}\right)e^{f(x)}. \tag{22}$$

With the approach of (18) it is possible to gauge transform (15). The first step

is to multiply equation (22) from the left with $i\hbar e^{-iS(\vec{x},t)}$, to get to the l.h.s of the Schrödinger equation,

$$i\hbar\frac{\partial}{\partial t}\psi = i\hbar e^{-iS(\vec{x},t)}\left[\frac{\partial}{\partial t} - i\frac{\partial S(\vec{x},t)}{\partial t}\right]e^{iS(\vec{x},t)}\psi. \tag{23}$$

The r.h.s gets transformed too,

$$\left(\hat{p} - \frac{e}{c}\vec{A}\right)^2 = \left(\frac{\hbar}{i}e^{-iS(\vec{x},t)}\left(\vec{\nabla} - i\vec{\nabla}S(\vec{x},t)\right)e^{iS(\vec{x},t)} - \frac{e}{c}\vec{A}\right)^2 =$$

$$= \left(\frac{\hbar}{i}e^{-iS(\vec{x},t)}\vec{\nabla}e^{iS(\vec{x},t)} - \frac{e}{c}\underbrace{\left(\vec{A} + \vec{\nabla}\Lambda(\vec{x},t)\right)}_{\vec{A}'}\right)^2 = \cdots = \tag{24}$$

$$= e^{-iS(\vec{x},t)}\left[-\hbar^2\vec{\nabla}^2 - \frac{\hbar}{i}\vec{\nabla}\vec{A}' - \frac{\hbar}{i}\vec{A}'\vec{\nabla}e^{iS(\vec{x},t)} + \left(\frac{e}{c}\vec{A}'\right)^2\right]e^{iS(\vec{x},t)} =$$

$$= e^{-iS(\vec{x},t)}\left[\frac{\hbar}{i}\vec{\nabla} - \frac{e}{c}\vec{A}'\right]^2 e^{iS(\vec{x},t)}. \tag{25}$$

Combining (23) with (25) and canceling out $e^{-iS(\vec{x},t)}$ leads to

$$i\hbar\left[\frac{\partial}{\partial t} - i\frac{\partial S(\vec{x},t)}{\partial t}\right]\underbrace{e^{iS(\vec{x},t)}\psi}_{\psi'} = \left(\frac{1}{2m}\left[\frac{\hbar}{i}\vec{\nabla} - \frac{e}{c}\vec{A}'\right]^2 + e\phi\right)\underbrace{e^{iS(\vec{x},t)}\psi}_{\psi'}. \tag{26}$$

Last, we have to rewrite (26) to get the complete gauge transformed Schrödinger equation

$$i\hbar\frac{\partial}{\partial t}\psi' = \left(\frac{1}{2m}\left[\frac{\hbar}{i}\vec{\nabla} - \frac{e}{c}\vec{A}'\right]^2 + e\underbrace{\left(\phi - \frac{1}{c}\frac{\partial\Lambda(\vec{x},t)}{\partial t}\right)}_{\phi'}\right)\psi'. \tag{27}$$

Stressing once more the gauge transformed wave function

$$\psi' = \psi e^{\frac{ie}{\hbar c}\Lambda(\vec{x},t)}, \tag{28}$$

we define the gauge transformation as

$$U \equiv e^{\frac{ie}{\hbar c}\Lambda(\vec{x},t)}. \tag{29}$$

Due to the fact the operator U is unitary ($U \in U(1)$), the physics is unchanged and all observable quantities are gauge invariant. [9]

This can easily be shown, by computing the expectation value of an arbitrary Hermitian operator $\mathcal{O}$ [2]

$$\langle \mathcal{O}' \rangle = \langle U\mathcal{O}U^{-1} \rangle = \int_{\mathbb{R}} \psi'^{*} U\mathcal{O}U^{-1}\psi' \mathrm{d}x =$$

$$= \int_{\mathbb{R}} \psi^{*} \underbrace{U^{-1}U}_{\hat{1}} \mathcal{O} \underbrace{U^{-1}U}_{\hat{1}} \psi \mathrm{d}x = \langle \mathcal{O} \rangle, \tag{30}$$

where $\mathcal{O}' = U\mathcal{O}U^{-1}$ is the gauge transformed $\mathcal{O}$.
Furthermore, we use the last argument to relate the Hamiltonian $\hat{H}_0$, which holds at a time where the magnetic flux is zero, to a time where the vector potential is present. [19]

$$i\hbar \frac{\partial}{\partial t}\psi = \hat{H}_0\psi \quad \Leftrightarrow \quad i\hbar \frac{\partial}{\partial t} U\psi = U\hat{H}_0U^{-1}U\psi \tag{31}$$

Rewriting (31) the Schrödinger equation takes the form

$$i\hbar \frac{\partial}{\partial t}\psi' = \hat{H}\psi' \ \text{ with } \ \hat{H} = U\hat{H}_0U^{-1} \tag{32}$$

Concluding this section, we have found that the phase of the gauge transformation U depends on the used gauge. [20]

1.3.3 Phase shift in a field-free-region

Consider a experiment where at first no magnetic field is used. Later on a constant magnetic flux is switched on adiabatically, but due to the chosen set-up it is enclosed to an impenetrable cylinder. Moreover, we wait long enough till

$$\vec{A}(\vec{x}, t) = \vec{A}(\vec{x}) \tag{33}$$

holds. This corresponds to a gauge transformation of the kind [8]

$$\vec{A}(\vec{x}) = \vec{A_0}(\vec{x}) + \vec{\nabla}\Lambda(\vec{x}) \ \text{ with } \ |\vec{A_0}| = 0. \tag{34}$$

The justification of that lies in

$$\vec{B} = 0 = \vec{\nabla} \times \vec{A} \ \Leftrightarrow \vec{A} = \vec{\nabla}\Lambda, \tag{35}$$

since the wave function of the electron cannot enter the regime of the magnetic field. [21]

Henceforth the gauge function $\Lambda(\vec{x})$ takes the form

$$\Lambda(\vec{x}) = \int_{\vec{x_0}}^{\vec{x}} \vec{A}(\vec{x}')\mathrm{d}\vec{x}', \tag{36}$$

where the integration is carried out on an arbitrary path in space. [21] If $\vec{B} = \vec{\nabla} \times \vec{A} = 0$, the line integral depends only on the beginning $\vec{x}_0$ and the ending $\vec{x}$, not on the path itself. [11, 13]

To give (36) meaning, we consider integrals of the form

$$\int_{\vec{x_0},\,1}^{\vec{x}} \vec{A}(\vec{x}')\mathrm{d}\vec{x} \quad \text{and} \quad \int_{\vec{x_0},\,2}^{\vec{x}} \vec{A}(\vec{x}')\mathrm{d}\vec{x}',$$

with 1 and 2 denoting different paths. These paths have the same starting and ending point and enclose therefore the surface σ. See Figure 3 for graphical interpretation. Next, one can use the magnetic flux through the specific surface σ,

$$\phi = \int_{\sigma} \vec{B} \cdot \mathrm{d}\vec{\sigma} \tag{37}$$

where σ is enclosed by the curve that path 1 and path 2 encircle. [21] Now we use the relation [12]

$$\vec{B} = \vec{\nabla} \times \vec{A}, \tag{38}$$

to get to

$$\int_{\sigma} \vec{B} \cdot \mathrm{d}\vec{\sigma} = \int_{\sigma} \left[\vec{\nabla} \times \vec{A}\right] \cdot \mathrm{d}\vec{\sigma}. \tag{39}$$

Stoke's theorem allows us to transform the surface integral to a line integral over the boundary of σ. [14]

$$\begin{aligned} \phi = \oint_{\partial\sigma} \vec{A} \cdot \mathrm{d}\vec{x}' = \int_{\vec{x_0},\,1}^{\vec{x}} \vec{A} \cdot \mathrm{d}\vec{x}' + \int_{\vec{x},\,2}^{\vec{x_0}} \vec{A} \cdot \mathrm{d}\vec{x}' \; = \\ = \int_{\vec{x_0},\,1}^{\vec{x}} \vec{A} \cdot \mathrm{d}\vec{x}' - \int_{\vec{x_0},\,2}^{\vec{x}} \vec{A} \cdot \mathrm{d}\vec{x}' \end{aligned} \tag{40}$$

In conclusion, it is important to note that path 1 and 2 encircle a shielded magnetic flux on different sides. The wave functions emitted at point $\vec{x}_0$ propagate either on path 1 or 2 and get detected on point $\vec{x}$. Due to their differing phases, they will interfere. As it turns out, this depends on the magnetic flux their paths encircle.

To generalize the discussion of phase shifts in regions where the magnetic field is absent, it is important to point out that analog methods can also be used for the electric case. Due to the 4-vector formulation of electrodynamics the 4-potential can be written as [12]

$$A_\mu(x) = (\phi(\vec{x}, t), -\vec{A}(\vec{x}, t)), \quad \text{with} \quad x = \{t, x, y, z\}. \tag{41}$$

The space-time line element which we need for integration looks like

$$\mathrm{d}x^\mu = (c\mathrm{d}t, \mathrm{d}\vec{x}). \tag{42}$$

With this generalization the electromagnetic flux takes the form

$$\frac{e}{\hbar c}\oint A_\mu(x)\mathrm{d}x^\mu = \frac{e}{\hbar c}\left[\oint c\phi(\vec{x},t)\mathrm{d}t - \oint \vec{A}(\vec{x},t)\mathrm{d}\vec{x}\right], \tag{43}$$

where the integration is carried out on a closed curve in space-time. [2]

1.3.4 Coulomb gauge

Since we are interested in the pure magnetic AB-effect, we choose

$$\phi(\vec{x},t) = 0 \tag{44}$$

and fix the gauge with the so-called Coulomb-gauge [19]

$$\vec{\nabla}\cdot\vec{A} = 0. \tag{45}$$

Additionally all our idealized problems show plane polar symmetry, and due to the choice $\vec{B} \parallel \hat{e}_z$ we expect $\vec{A} \parallel \hat{e}_\theta$. Therefore, the following integration can be carried out [1]

$$\phi = \oint \vec{A}(\vec{x})\mathrm{d}\vec{x} = \int_0^{2\pi} A_\theta \rho \mathrm{d}\theta = 2\pi\rho A_\theta. \tag{46}$$

It follows that

$$\vec{A}(\theta,\rho) = \frac{\phi}{2\pi\rho}\hat{e}_\theta. \tag{47}$$

This choice as well satisfies the Coulomb-condition

$$\vec{\nabla}\cdot\vec{A} = \frac{1}{\rho}\frac{\partial}{\partial\theta}\frac{\phi}{2\pi\rho} = 0 \tag{48}$$

and represents a suitable function for the the vector potential, since it vanishes at $\rho \to \infty$. $\vec{A} \neq \vec{A}(\theta)$ exhibits once more polar symmetry.

1.4 Bound state problem

Before we deal with experimental set-ups and interference it is very revealing to take a look on the bound state AB-effect. This shows at least mathematically the influence of the vector potential $\vec{A}$ on an electron. Consider the set-up shown

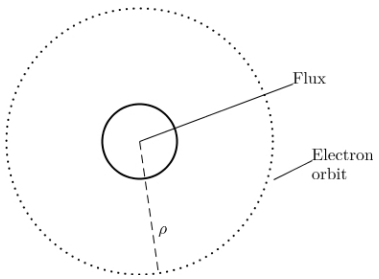

Figure 1: Electron orbiting magnetic flux [19]

in Figure 1, where an electron encircles a solenoid on a one-dimensional wire with radius ρ. Assuming the solenoid's length infinite, guarantees $\vec{B} = 0$ on the outside of the cylinder. Without loss of generality we, choose $\vec{B} \| \hat{e}_z$, so $\phi > 0$. Due to the cylindrical symmetry we use polar coordinates with the azimutal angle θ. Here, the Schrödinger equation takes the form [13, 19, 21]

$$\frac{1}{2m}\left[\frac{\hbar}{i}\vec{\nabla} - \frac{e}{c}\vec{A}\right]^2 \psi(\theta) = \frac{1}{2m}\left[-i\hbar\frac{1}{\rho}\frac{\partial}{\partial\theta} - \frac{e}{c}A_\theta\right]^2 \psi(\theta) =$$

$$= \frac{\hbar^2}{2m\rho^2}\left[-\frac{\partial^2}{\partial\theta^2} + i2\frac{e}{c\hbar}\frac{\phi}{\pi}\frac{\partial}{\partial\theta} + \left(\frac{e}{\hbar c}\frac{\phi}{2\pi}\right)^2\right]\psi(\theta) = E\psi(\theta). \tag{49}$$

The factor of 2 at the single derivative ∂_θ arises due to the commutator

$$[\partial_\theta, A_\theta]\,\psi(\theta) = \partial_\theta\left(A_\theta\psi(\theta)\right) - A_\theta\partial_\theta\psi(\theta) = \psi(\theta)\partial_\theta A_\theta = 0. \tag{50}$$

$$\implies \partial_\theta\left(A_\theta\psi(\theta)\right) = A_\theta\partial_\theta\psi(\theta) \tag{51}$$

To write (49) more transparently we define $\phi_0 \equiv \frac{\pi}{e}\hbar c$ and rewrite

$$\frac{\partial^2\psi(\theta)}{\partial\theta^2} - i2\underbrace{\frac{\phi}{\phi_0}}_{\equiv\beta}\frac{\partial\psi(\theta)}{\partial\theta} + \underbrace{\left(\frac{2mE\rho^2}{\hbar^2} - \underbrace{\frac{\phi^2}{\phi_0^2}}_{\equiv\beta^2}\right)}_{\equiv\epsilon}\psi(\theta) = 0 \tag{52}$$

This ordinary differential equation with constant coefficients is solved by the wave ansatz [13]

$$\psi(\theta) = Ce^{i\lambda\theta}, \tag{53}$$

$$\text{with } \lambda = \beta \pm \sqrt{\beta^2 + \epsilon} = \frac{\phi}{\phi_0} \pm \frac{\rho}{\hbar}\sqrt{2mE}. \tag{54}$$

To specify the parameter λ, we have to consider the continuity of the wave function at $2\pi \rightarrow 0$.

$$\psi(2\pi) = \psi(0) \quad \Rightarrow \quad 1 = e^{i2\pi\lambda} \tag{55}$$

From equation (55) follows that λ has to be integer, we call it l. Furthermore, ψ has to be normalized to 1 so C becomes

$$\int_0^{2\pi} \mathrm{d}\theta |Ce^{il\theta}|^2 = 1 \quad \Rightarrow \quad C = \frac{1}{\sqrt{2\pi}} \tag{56}$$

Now the complete wave function is [19]

$$\psi(\theta) = \frac{1}{\sqrt{2\pi}} e^{il\theta} \tag{57}$$

With the computed wave function, the energy spectrum becomes

$$\frac{\hbar^2}{2m\rho^2}\left[-i\frac{\partial}{\partial\theta} - \frac{\phi}{\phi_0}\right]^2 \psi(\theta) = \frac{\hbar^2}{2m\rho^2}\left[l - \frac{\phi}{\phi_0}\right]^2 \psi(\theta) = E_l\psi(\theta). \tag{58}$$

$$E_l = \frac{\hbar^2}{2m\rho^2}\left[l - \frac{\phi}{\phi_0}\right]^2 = \frac{\hbar^2}{2m\rho^2}\left[l - \frac{e\phi}{2\pi\hbar c}\right]^2 \quad \text{with } \; l \in \mathbb{Z} \tag{59}$$

Thus, the energy spectrum of the bound states depends directly on the magnetic flux, though the magnetic field is zero outside of the solenoid. Considering positive l as counterclockwise and in contrary negative l as clockwise rotations, we can interpret equation (59). If the particle orbits the solenoid counterclockwise with a certain l, the energy would be higher (since $e = -e_0 < 0$), in comparison to the opposite case. [13]

The calculation above can be generalized, by allowing the electron to move in a radially symmetric potential $V(\rho)$ around the magnetic flux, which is shielded by a barrier or impenetrable cylinder. The main conclusion of this slightly sophisticated problem reveals once more that the energy spectrum depends on the enclosed magnetic flux. [8]

The value of the introduced constant $2\phi_0$ is in Gaussian units [20]

$$2\phi_0 = \frac{2\pi\hbar c}{e} = \frac{hc}{e} = 4.135 \times 10^{-7}\text{Gauss cm}^2 \tag{60}$$

and has further physical interpretation. For reasons that will come up later in this discussion, the introduced constant is the named "fundamental unit of magnetic flux".

1.5 Interference Experiments with e.m. potentials

To understand the upcoming experimental set-ups, it is very important to clarify the general concept of interference experiments which are designed to show the influence of electromagnetic potentials on electrons.

Interference in general occurs at the superposition of waves. That argument holds for light waves, as well as for electron waves. Furthermore, to get stationary fringes (interference pattern), the superposed waves have to be coherent. Two superposed waves are coherent if their time-dependent wave functions are equal except for a phase difference $\Delta\varphi$,

$$\psi_1(t) = \text{const.} \times \psi_2(\omega t + \Delta\varphi). \tag{61}$$

If the wave packets do not spatially overlap, there is no way that they can interfere. [15]

Therefore, one important feature of interference experiments is to create time-independent fringes. To achieve such interference patterns, one can either use set-ups that create stationary fringes anyway and add electromagnetic flux as perturbation, or use the pure electromagnetic potentials themselves instead. But it is very challenging to arrange such experiments, because the electrostatic potential ϕ and the vector potential $\vec{A}$ have to be separated carefully from the electromagnetic fields $\vec{E}$ and $\vec{B}$.

1.5.1 Double slit

For better understanding of Aharonov and Bohm's attempt, it is possible to illustrate the influence of vector potential using a double slit experiment. Figure 1 shows a classical double slit experiment. The continuous line represents the outcome of the experiment if no magnetic flux is present, while the dashed line

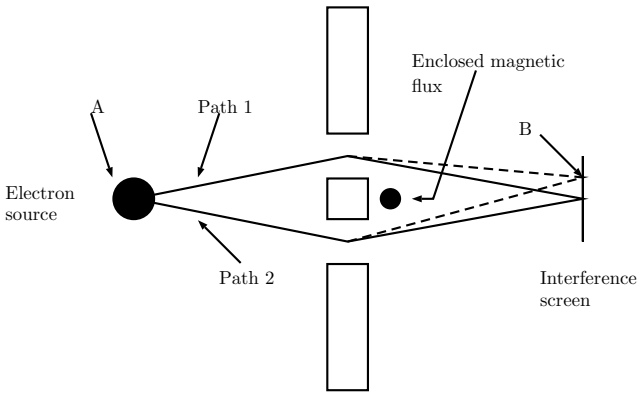

Figure 2: Double slit experiment [9]

suggests interaction between the vector potential and the electron.

As shown in section 1.3.3 the wave function in a region with a non-zero vector potential $\vec{A}$ is

$$\psi = \psi_0 e^{\frac{ie}{\hbar c}\int \vec{A}(\vec{x})\mathrm{d}\vec{x}} \tag{62}$$

where ψ_0 represents the free case wave function. At first, to compute the interference pattern, we close one of the slits and arrange the wave functions. [21]

$$\psi_1 = \psi_{1,0} e^{\frac{ie}{\hbar c}\int_1 \vec{A}(\vec{x})\mathrm{d}\vec{x}} \tag{63}$$

$$\psi_2 = \psi_{2,0} e^{\frac{ie}{\hbar c}\int_2 \vec{A}(\vec{x})\mathrm{d}\vec{x}} \tag{64}$$

The final result for both slits open arises at the superposition of (63) and (64),

$$\Psi = \psi_1 + \psi_2 = \psi_{1,0} e^{\frac{ie}{\hbar c}\int_1 \vec{A}(\vec{x})\mathrm{d}\vec{x}} + \psi_{2,0} e^{\frac{ie}{\hbar c}\int_2 \vec{A}(\vec{x})\mathrm{d}\vec{x}}. \tag{65}$$

Next we extract the phase factor of ψ_2 and this leads to

$$\Psi = \left[\psi_{1,0} e^{\frac{ie}{\hbar c}\left[\int_1 \vec{A}(\vec{x})\mathrm{d}\vec{x} - \int_2 \vec{A}(\vec{x})\mathrm{d}\vec{x}\right]} + \psi_{2,0}\right] e^{\frac{ie}{\hbar c}\int_2 \vec{A}(\vec{x})\mathrm{d}\vec{x}}. \tag{66}$$

Stressing the calculations we did in section 1.3.3, the complete wave function can be written as [21]

$$\Psi = \left[\psi_{1,0} e^{\frac{ie}{\hbar c}\phi} + \psi_{2,0}\right] e^{\frac{ie}{\hbar c}\int_2 \vec{A}(\vec{x})\mathrm{d}\vec{x}}. \tag{67}$$

Using equation (67) we can write down the probability density P. [21]

$$P = |\Psi|^2 = \Psi\Psi^* =$$

$$= \left[\psi_{1,0} e^{\frac{ie}{\hbar c}\phi} + \psi_{2,0}\right] e^{\frac{ie}{\hbar c}\int_2 \vec{A}(\vec{x})\mathrm{d}\vec{x}} \times \left[\psi_{1,0} e^{\frac{ie}{\hbar c}\phi} + \psi_{2,0}\right]^* e^{-\frac{ie}{\hbar c}\int_2 \vec{A}(\vec{x})\mathrm{d}\vec{x}} =$$

$$= |\psi_{1,0}|^2 + |\psi_{2,0}|^2 + 2Re\left(\psi_{1,0}^* \psi_{2,0} e^{-\frac{ie}{\hbar c}\phi}\right) \tag{68}$$

Summing up the last calculations, it is important to note that the shift of the interference pattern depends numerically on the enclosed magnetic flux. This set-up should approximately show how interference pattern are shifted if a magnetic flux is switched on. Though for computing the AB-wave functions, it is not important to add a double slit to the experiment, as we will see in the next section. [3] Using a double slit, however, is illustrative because the wave functions take the form of cylindrical waves. [21]

1.5.2 Aharonov-Bohm-set-up

For showing the magnetic AB-effect Aharonov and Bohm suggested the following experimental setting:

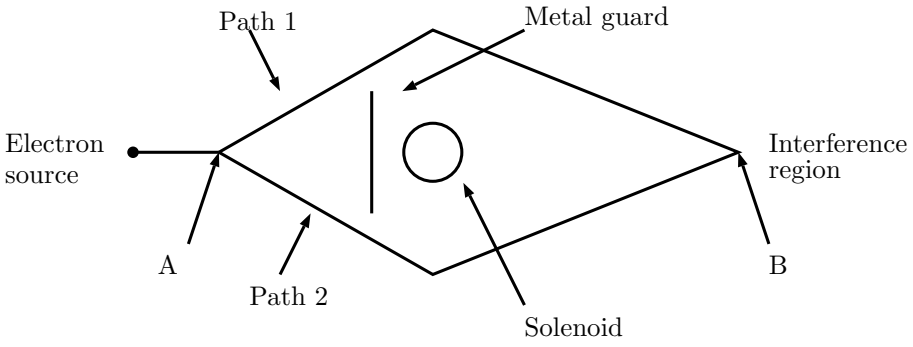

Figure 3: Interference Experiment in the sense of Aharonov and Bohm [1]

Figure 3 is just a schematic representation of actually realized experiments, but it can be used for the calculation of the phase shift. The technical details to arrange such experimental set-ups will be discussed in section "AB-Effect: Experiments".

As can be seen in the figure, the electrons are emitted by a source. At point A the beam is split coherently, to focus it later on to point B, where the interference pattern can be observed. [19] On their paths (1 or 2) the electrons are fully shielded of the magnetic field. Because (i) the magnetic field of the infinite solenoid exists only on its inside [12] and (ii) the metal guard is arranged in a way no electron can enter the inside of the solenoid. The assumption that the solenoid is infinite, can actually be realized if the magnetic flux is enclosed by an impenetrable cylinder. [20]

The fact that the magnetic field of the solenoid vanishes on the outside and is constant on the inside, shows that the vector potential $\vec{A}$ cannot vanish everywhere. [19]

Similar to the wave function in section 1.5.1, one can arrange the general AB-wave function like this:

$$\Psi = \left[\psi_{1,0} e^{\frac{ie}{\hbar c}\phi} + \psi_{2,0}\right] e^{\frac{ie}{\hbar c}\int_2 \vec{A}(\vec{x})\mathrm{d}\vec{x}}, \tag{69}$$

where $\psi_{1,0}$ and $\psi_{2,0}$ represent the undisturbed wave function on paths 1 and 2. [3] In general, this problem is not trivial, so Aharonov and Bohm simplified the calculation by setting the radius of the flux line to zero. Therefore, the AB-effect reduces to an incoming plane electron wave that gets scattered at the flux line. [1]

1.6 Scattering AB-effect

To obtain exact solutions for the scattering states, Aharonov and Bohm fixed the flux, but assumed a vanishing radius. The associated stationary Schrödinger equation in cylindrical coordinates takes the form [1]

$$\left[\frac{1}{2m}\left[\frac{\hbar}{i}\vec{\nabla}-\frac{e}{c}\vec{A}\right]^2+e\phi(\vec{x})\right]\psi=\cdots=$$

$$=\left[\frac{\partial^2}{\partial\rho^2}+\frac{1}{\rho}\frac{\partial}{\partial\rho}+\frac{1}{\rho^2}\left(\frac{\partial}{\partial\theta}+i\alpha\right)^2+k^2\right]\psi=0. \tag{70}$$

Where $\vec{k}$ is the wave vector,

$$|\vec{k}|=k=\frac{1}{\hbar}\sqrt{2mE}, \tag{71}$$

and a flux parameter

$$\alpha=-\frac{e\phi}{ch}. \tag{72}$$

In the limit of vanishing flux-radius, it is justified to assume the incoming wave function as a single plane wave [1]

$$\psi_0=e^{-i\vec{k}\vec{x}}=e^{-ik\rho\cos\theta}. \tag{73}$$

Due to the gauge transformation (29), we are able to compute the disturbed plane wave ψ,

$$\psi=e^{-ik\rho\cos\theta}e^{\frac{ie}{\hbar c}\int_{\vec{x}_0}^{\vec{x}}\vec{A}(\vec{x}')\mathrm{d}\vec{x}'}. \tag{74}$$

Combining (72) and the Coulomb-gauge condition, the integral in the phase can be computed

$$\int_{\vec{x}_0}^{\vec{x}}\vec{A}(\vec{x}')\mathrm{d}\vec{x}'=\int_0^{\theta}A_\theta\mathrm{d}\theta=\frac{\phi}{2\pi}\theta \tag{75}$$

and the wave function takes the form [3]

$$\psi=e^{-ik\rho\cos\theta}e^{-i\alpha\theta}. \tag{76}$$

It is obvious that (76) does not fulfill the condition $\psi(\rho=0)=0$, but, as we will see later on, this is a special case for integer α and has to be treated separately. Furthermore, diffraction has not been considered. Aharonov and Bohm stated that this contribution can be neglected. [1] In the end, equation (76) is a correct incoming wave function for this problem.

The next step is, to compute the exact scattering states Ψ. We expand the wave function ψ in partial waves, in eigenstates of the angular momentum operator. [3, 21]

We find that the AB-wave function is proportional to a superposition of positive order Bessel-functions $J(k\rho)_{|l+\alpha|}$. [1]

$$\Psi = \sum_{l=-\infty}^{\infty} (-i)^{|l+\alpha|} J_{|l+\alpha|}(k\rho) e^{il\theta} \tag{77}$$

The achievement of Aharonov and Bohm was the interpretation of Ψ. They converted the exact wave function to a manageable form of [21]

$$\Psi = e^{-i\vec{k}\vec{x}} + \frac{e^{\pm ik\rho}}{\sqrt{r}} f(\theta). \tag{78}$$

Now one can read off the scattered wave function and the scattering amplitude $f_{\vec{k}}(\theta)$. The general solution takes the form [1] [19]

$$\Psi = e^{-i\vec{k}\vec{x}} + \frac{e^{ik\rho}}{\sqrt{2\pi ikr}} \sin\pi\alpha \frac{e^{-i\frac{\theta}{2}}}{\cos\frac{\theta}{2}}. \tag{79}$$

The scattering amplitude reads off as

$$f(\theta) = \frac{\sin\pi\alpha}{\sqrt{2\pi i}} \frac{e^{-i\frac{\theta}{2}}}{\cos\frac{\theta}{2}}. \tag{80}$$

With the resulting scattering amplitude, we are able to compute the differential scattering cross section [21]

$$\frac{\mathrm{d}\sigma}{\mathrm{d}\Omega} = |f(\theta)|^2 = \frac{1}{2\pi} \frac{\sin^2\pi\alpha}{\cos^2\frac{\theta}{2}}. \tag{81}$$

1.6.1 Integer α

Consider now

$$\alpha = n, \;\; n \in \mathbb{Z}. \tag{82}$$

With this assumption, $\sin\pi n = 0, \;\; \forall\, n \in \mathbb{Z}$ and (76) takes the form

$$\Psi = e^{-i\vec{k}\vec{x}}. \tag{83}$$

This means that there is no observable effect on the electron wave - no interference - if the flux is quantized by integral numbers. [19]

However, this actually is already revealed by the very general equation (68), where the interference pattern is determined by the phase factor $e^{\frac{ie}{\hbar c}\phi}$. Rewriting the phase factor leads to vanishing interference

$$e^{\frac{ie}{\hbar c}\phi} = e^{\frac{2\pi ie}{hc}\phi} = e^{-i2\pi\alpha} = e^{-i2\pi n} = 1. \tag{84}$$

In other words: (83) is a correct wave function for this case and it is not important if it vanishes at $\rho = 0$ or not, because there is no observable effect anyway.

1.6.2 Half-integer α

The second exact solvable case is

$$\alpha = n + \frac{1}{2},\ n\ \in\ \mathbb{Z}. \tag{85}$$

A closer look on equation (80) reveals that the interference is at a maximum in the half-integer case. Due to the fact that there are observable effects, one has to deal with the full wave function (77).

To show that Ψ is a correct wave function for this problem, one has to remember the definition of the Bessel-functions, [14]

$$J_p(k\rho) = \sum_{n=0}^{\infty} \frac{(-1)^n}{\Gamma(n+1)\Gamma(n+p+1)} \left(\frac{k\rho}{2}\right)^{2n+p}. \tag{86}$$

Since p is equal to $|l + n + \frac{1}{2}|$ and l as well as n are integer, p is half-integer. Therefore, all Bessel-functions vanish at the origin.

In the limit of a vanishing radius of the flux tube, the wave function vanishes at $\rho = 0$. Now it is possible to introduce a shield potential to fully protect the electron of the magnetic flux. The wave function will however remain the same, as long as the radius of the shield vanishes too.

The exact wave function that was computed by Aharonov and Bohm, takes the form

$$\Psi = \sqrt{\frac{i}{2}} e^{-i\left(\frac{1}{2}\theta + k\rho\cos\theta\right)} \int_0^{\sqrt{k\rho(1+\cos\theta)}} e^{iz^2} \mathrm{d}z. \tag{87}$$

Using the relation [1]

$$\lim_{\tau\to+\infty} \int_0^{\tau} e^{iz^2} \mathrm{d}z \ \longrightarrow\ \frac{i}{2}\frac{e^{i\tau^2}}{\tau} \tag{88}$$

and the resulting wave function, one can compute the scattering amplitude in the limit $\rho \to \infty$, [19]

$$f(\theta) \propto \frac{e^{-i\frac{\theta}{2}}}{\cos\frac{\theta}{2}}. \tag{89}$$

Now we can deduce the differential scattering cross section

$$\frac{\mathrm{d}\sigma}{\mathrm{d}\Omega} \propto \frac{1}{\cos^2\frac{\theta}{2}}. \tag{90}$$

As expected, is the asymptotic behavior of the exact wave function related to the general solution (80).

1.7 Single-valuedness of Ψ

In previous sections we calculated solutions for problems, implying excluded flux regions, though spared an important issue: Is the solution of the Schrödinger equation still meaningful if it is computed in regions, where parts of space are missing?

Requiring a vanishing wave function in the flux region is strongly associated with excluding regions that are in the domain of the wave function. That leads, mathematically spoken, to a multiply-connected region. As we have seen in previous sections, the wave function gains a phase by propagating in such regions.

That the initial wave function

$$\Psi = e^{-ik\rho\cos\theta}e^{-i\alpha\theta} \tag{91}$$

is multivalued, can easily be shown by leading the wave function one time on a circuit around the excluded soleniod. [3] The change of the wave function is therefore

$$e^{-i2\pi\alpha}. \tag{92}$$

It vanishes only if α is integer and from that follows the wave function is automatically single-valued. Since (90) is in general not a useful wave function it, is reasonable to consider this special case only.

For the second exact solvable case, α is half-integer, the wave function is also single-valued. [1] This property is not as obvious as in the first case. The reason for single-valuedness is the asymptotic behavior of (87). It is the same as the general solution (79), for half-integer flux parameter α, as shown in section 1.6.2. [19]

Generally, it is important to note that due to the single-valuedness of the Hamiltonian, the single-valuedness of a wave function is preserved. If a wave function is single-valued in the first place (in our case far from the origin), this property cannot be changed. [2]

2 AB-Effect: Experiments

2.1 Chambers [4]

A few months after Aharonov and Bohm published their first paper, Robert G. Chambers realized the first experiment focusing on the AB-effect. The following experimental set-up was used: A and B denote the different electrodes of

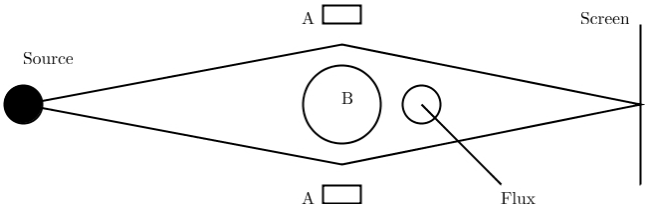

Figure 4: Chambers' interference experiment [4]

an electron-biprism, which was used to focus the electrons to the observation screen. The electrodes A are used as groundings, whereas B provides a positive potential that determines the angle of deflection. In the shadow of B a mono-crystalline iron filament, with a diameter of 1 μm, is arranged. This so-called iron whisker [23] is partly conical and partly cylindrical and provides the magnetic flux. Since the magnetic domains in this whisker are uniform, the flux direction is well-defined. [19]

Further it is interesting to note that the whisker tapers approximately constant with a slope of 10^{-3} rad. Stressing this fact and the uniformity of the magnetization, one finds that the enclosed flux decreases with the length of the filament This means that the phase of the electrons depends highly on the point of passing. [18]

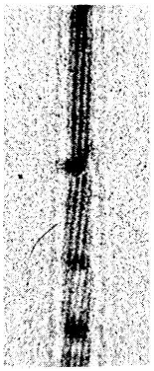

Figure 5: Tilted fringes caused by conical whisker [4]

Additionally, it is known that the magnetic lines exit the tapered parts of the whisker perpendicular to the surface. Therefore, a stray field exists, which tilts the interference fringes proportionally to the flux change. Additionally to the tilt, the fringes are continuously connected. This holds if the phase shift exists in the cylindrical regime too. [19]

In conclusion it has to be mentioned that there has been criticism too. Aharonov and Bohm stated that the use of whiskers does not provide a solid proof of the AB-effect, since $\vec{A}$ and $\vec{B}$ are not separated adequately. [2]

2.2 Möllenstedt and Bayh [16]

In 1962 the second remarkable experiment was carried out by G. Möllenstedt and W. Bayh. They used a similar set-up like Chambers, as can be seen in Figure 4, but in contrary a thin solenoid was used to generate the magnetic flux. To minimize the leakage fields, a Fe/Ni-frame was added to the solenoid,

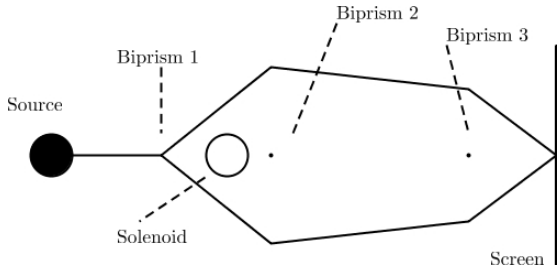

Figure 6: Interference experiment of Möllenstedt and Bayh, [16]

which was made of tightly wound Wolfram-wire. The purpose of such a frame, was to short-circuit the magnetic field on the ends of the solenoid. Furthermore, they stated that such a set-up is preferable to the use of whiskers, because the flux is not fixed to the filament. This property was stressed to visualize the consequences of the vector potential.

As the solenoid current was increased up to 0.8 μA, a film was moved proportionally to the current change. The outcome of the experiment is shown in Figure 5, where the fringe shifts, which appear due to the vector potential, are visible. The analysis of the experiment confirmed furthermore the modulus of the flux quantum

$$\phi_0 = 4.07 \times 10^{-7} Gcm^2 \pm 14\%.$$

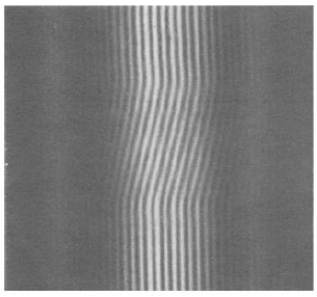

Figure 7: Interference pattern with fringe shifts [16]

2.3 Tonomura et al. I [5]

The next experiment was carried out in 1982 by Akira Tonomura et al. They chose a different set-up as Chambers or Möllenstedt and Bayh, namely optical- and electron-holography. This technique consists of two parts, an electron microscope and an optical system, which transforms the electron waves into light waves. [22] In Figure 8 the setting for the electron microscope is sketched. In the case of the actual experiment, the "Specimen" is realized by a toroidal Fe/Ni-alloy, with an outer radius of about 1 μm. The advantage of a toroidal shaped magnet, is the reduction of leakage fields. Since the magnetization could be orientated clockwise or counterclockwise, the flux is by approximation confined to the magnet. More precisely, one of the consequences of this experiment was showing that the leakage fields were too small to affect the AB-phase.

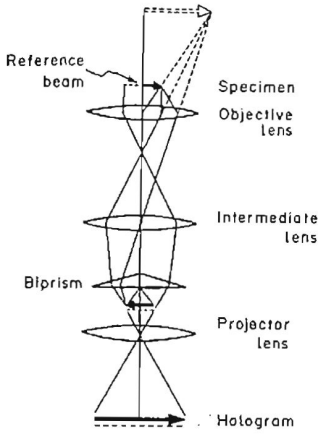

Figure 8: Set-up for electron holography [5]

Figure 9 shows the second part of the set-up, which was used to reconstruct the electron hologram. The beams were provided by a He-Ne laser and then split coherently into two beams. The first beam pictures the hologram of the toroidal magnet, whereas the second was used as "reference" to get the interference pattern. Since this method only magnifies the signal, the amplitude and phase of the electron wave is conserved and the image of the torus is meaningful. [22]

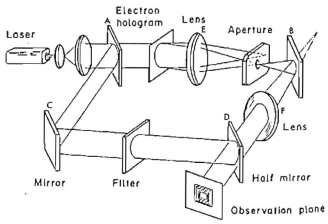

Figure 9: Set-up for Reconstruction of electron hologram [5]

Figure 10 shows an image of the torus, using two different methods. (a) is a so-called contour map of the electron phase, which was created by plane light wave parallel to the electron wave. It represents the magnetic lines inside the toroidal magnet. (b) on the contrary displays the interference pattern of the electron wave.

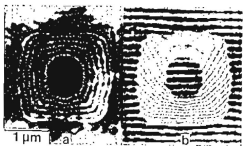

Figure 10: Interference pattern of the torus. (a) Contour map of the electron phase. (b) Interference pattern of the electron phase [5]

It shows the gained phase shift, due to the vector potential. This method is slightly different to the contour mapping. The electron hologram is imaged by a wave front, which is not parallel to the object wave. [22]

Shown are these differing techniques in Figure 11, where the labels match with Figure 10. This problem is comparable with a photograph of a mountain, where (a) is taken from above and (b) of the side. [22]

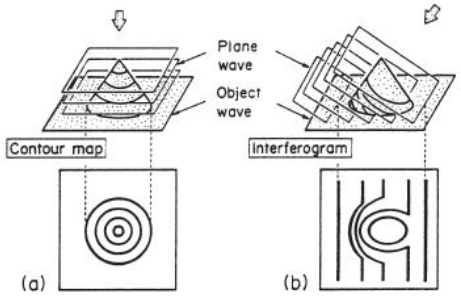

Figure 11: [22]

To summarize the first experiment of Tonomura et al., they showed that there exists a measurable effect due to the vector potential, because the electron waves that passed on different sides of the magnet, gained a visible phase difference. Furthermore, they performed a reasonable analysis of leakage fields and stated that the effect is too small to influence the interference experiments. [5]

2.4 Tonomura et al. II [6]

For further observation of the AB-effect, Tonomura et al. did a rerun of their experiment in 1986. Instead of using a bare toroidal magnet, they covered it with superconducting material, namely Niobium (Figure 12). By using such a set-up, they stressed the Meissner-Ochsenfeld-effect to increase the precision.

Due to circulating currents in layers near the surface, the magnetic field cannot fully penetrate the superconducting materials, if they are cooled under their critical temperature. [15] The consequences are twofold: on the one hand, the flux is conserved to the Fe/Ni-alloy and no leakage fields can influence the electron waves and on the other hand, the magnet is completely shielded by the Niobium, so the electrons cannot enter the regime of the Fe/Ni-torus.

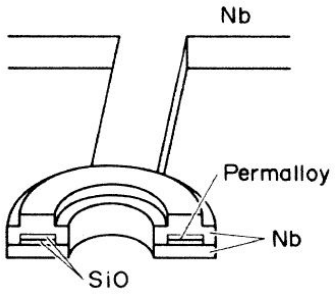

Figure 12: Diagram of the magnet structure [6]

Furthermore, it is interesting to visualize the thickness of the toroidal magnet. In Figure 12 it can be seen that the structure contains a SiO- and a Fe/Ni-layer.

The alloy is 20 nm, whereas the Silicon Monoxide-layer is 50 nm thick. Enclosed are these rings by 250 nm of Niobium and further by a additional 100 nm Cu-cover. Due to the approximated penetration depth of the electrons of 110 nm in Nb, it is very important to add further covering of the flux, to minimize the effects of leakage fields. They stated that at room temperature the magnitude of the leakage fields is of the order of approximately $h/20e$. Therefore, it is reasonable to assume the leakage fields at working temperature ($\ll$ 300K) much lower.

To conclude this section, it is interesting to analyze interferograms (see Figure 11) of the magnet.

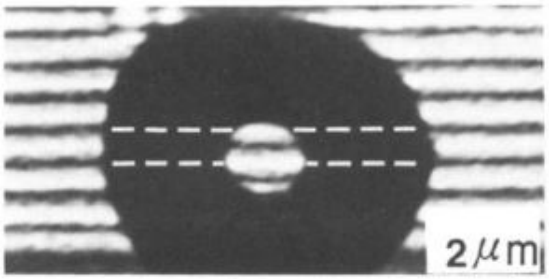

Figure 13: Interferogram of the toroidal magnet, T = 4.5K [6]

In Figure 13 the phase shift of the electron waves is visible. The electrons, which pass through the hole of the torus, gain a different phase than the ones, which pass on the outside. This is indicated by the dashed line.

One more time Tonomura et al. observed phase shifts, but under tightened conditions, compared to the experiment in 1982. Furthermore, they stated that the phase shift shown in Figure 13 is a multiple of π. This is an indication for flux quantization proportionally to $hc/2e$. (see equation 60)

3 Quantum Interference devices

3.1 AB-Effect in ring structures

In previous sections, we analyzed theoretical concepts, respectively experimental set-ups and noted the largeness of the particular electron microscopes or optical settings. An approach - not untypical for modern physics - is to minimize the existing structures and examine the consequences. That leads to the simplest toy-model, the Aharonov-Bohm-ring [AB-ring].

Figure 14: Experimental realization [17]

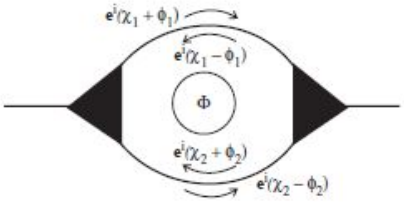

Figure 15: AB-ring [17]

Figure 14 shows an actually realized ring structure, where the black domains represent electron reservoirs. Figure 15 on the other hand, shows a sketch of an AB-ring, where the black colored triangles denote ideal beam splitters, which are described by a scattering matrix. Further, it is evident in the figure that two different phases are applied to the wave function if it passes trough on of the arms of the ring. χ_i is a dynamical phase, due to the device, and ϕ_i (i = 1,2) a magnetic phase, due to the flux. Since we consider only ideal rings, it is justified to choose $\chi_1 = \chi_2 = \chi/2$. [17]

For computing the transmission amplitude T, in fact every possible trajectory through the ring has to be counted. Considering only trajectories with a maximum of one loop, we end up with

$$T = \frac{(1-\cos\chi)(1+\cos\phi_{AB})}{\sin^2\chi + \left[\cos\chi - (1+\cos\phi_{AB})/2\right]^2}, \tag{93}$$

where $\phi_1 + \phi_2 = \phi_{AB} \equiv \frac{e}{\hbar c}\phi = \pi\frac{\phi}{\phi_0}$. [60] Using equation (93), it is possible to compute the conductance of an AB-ring. Generally, this is given by

$$G = G_Q T(\chi, \phi_{AB}) = \frac{e^2}{\pi\hbar} T(\chi, \phi_{AB}), \tag{94}$$

where G_Q is the conductance quantum. Summing up the last results, it follows that the conductance of the AB-ring alters periodically with ϕ_0 and therefore the resistance alters too. [17] This statement has been proven by many experiments with AB-like [17] and graphene rings. [7]

References

[1] Y. Aharonov and D. Bohm. Significance of electromagnetic potentials in the quantum theory. *Physical Review*, 115(3):485, August 1959.

[2] Y. Aharonov and D. Bohm. Further considerations on electromagnetic potentials in the quantum theory. *Physical Review*, 123(4):1511, August 1961.

[3] M.V. Berry. Exact Aharonov-Bohm wavefunction obtained by applying Dirac's magnetic phase factor. *European Journal of Physics*, 1:240–244, 1980.

[4] R. G. Chambers. Shift of an electron interference pattern by enclosed magnetic flux. *Physical Review Letters*, 5(1):3–5, July 1960.

[5] A. Tonomura et al. Oberservation of Aharonov-Bohm effect by electron holography. *Physical Review Letters*, 48(21):1443, May 1982.

[6] A. Tonomura et al. Evidence for Aharonov-Bohm effect with magnetic field completely shielded form electron wave. *Physical Review Letters*, 56(8):792, February 1986.

[7] J. Schelter et al. The Aharonov-Bohm effect in graphene rings. *arXiv:1201.6200 [cond-mat.mes-hall]*, January 2012.

[8] M. Peshkin. et al. The quantum mechanical effects of magnetic fields confined to inaccessible regions. *Annals of Physics*, 12(3):426–435, 1961.

[9] B. Felsager. *Geometry, Particles and Fields*. Odense University Press, 2 edition, 1983.

[10] R. Feynman. *Quantum Mechanics*, volume 3. Basic Books, 2010.

[11] T. Fliessbach. *Mechanik*. Spektrum, 6 edition, 2009.

[12] T. Fliessbach. *Elektrodynamik*. Spektrum, 6 edition, 2012.

[13] D.J. Griffiths. *Introduction to Quantum Mechanics*. Prentice Hall, 1995.

[14] C.B. Lang and N. Pucker. *Mathematische Methoden in der Physik*. Spektrum, 2 edition, 2010.

[15] D. Meschede. *Gerthsen Physik*. Springer-Verlag, 24 edition, 2010.

[16] G. Möllenstedt and W. Bayh. Kontinuierliche Phasenverschiebung von Elektronenwellen im kraftfeldfreien Raum durch das Vektorpotential eines Solenoids. *Physikalische Blatter*, 18(7):299–305, Juli 1962.

[17] Y.V. Nazarov and Y.M. Blanter. *Quantum Transport: Introduction to Nanoscience*. Cambridge University Press, 2009.

[18] S. Olariu and I. Iovitzu Popescu. The quantum effects of electromagnetic fluxes. *Reviews of Modern Physics*, 57(2):339–433, April 1985.

[19] M. Peshkin and A. Tonomura. *The Aharonov-Bohm Effect*. Springer-Verlag, 1989.

[20] J.J. Sakurai. *Modern Quantum Mechanics*. Addison-Wesley Publishing Company, revised edition edition, 1994.

[21] F. Schwabl. *Quantenmechanik*. Springer-Verlag, 7 edition, 2007.

[22] A. Tonomura. *Electron Holography*. Springer, 2 edition, 1999.

[23] Online version of McGraw-Hill Encyclopedia of Science and Technology.